Kriging metamodels for 2D finite element simulations of the settlements induced by TBM excavation in urban areas

Boris Kratz[1,2,3], Pierre Jehel[2], Maxime Tatin[2], Emmanuel Vazquez[1]

[1] Université Paris-Saclay, CNRS, CentraleSupélec, L2S - Laboratoire des signaux et systèmes, 91190, Gif-sur-Yvette, France

[2] Université Paris-Saclay, CentraleSupélec, ENS Paris-Saclay, CNRS, LMPS - Laboratoire de Mécanique Paris-Saclay, 91190, Gif-sur-Yvette, France

[3] Socotec Monitoring France, 91120, Palaiseau, France

Corresponding author: Boris Kratz (e-mail: boris.kratz@centralesupélec.fr)

ABSTRACT

The finite element method (FEM) is a classical approach to simulate the surface settlements induced by a tunnel boring machine (TBM). Unfortunately, for this application, the FEM is also computationally demanding. In this case, it is often useful to build simplified models from a set of reference simulations to quickly predict quantities of interest (QoIs) and make decisions. Such simplified models are called metamodels. In this article, our objective is to use kriging metamodels, aka Gaussian process metamodels, to build an approximation of a parametric 2D finite element tunneling model implemented using Python and ABAQUS. Our methodology evaluates the performance of kriging metamodels when the number of reference simulations varies. The performances are evaluated using several comparison metrics. We also compare two open-source implementations for kriging, two different assumptions for the mean of the Gaussian process, and we also test kriging against several classical regression methods.

Keywords FEM, Tunnelling, Metamodel, Settlements, Kriging

I. INTRODUCTION

Urban densification drives the need to expand underground networks. Monitoring in these hazardous environments is a major challenge for the building and civil engineering sector particularly for predicting surface settlements caused by tunnel excavation. Among other excavation methods, tunnel boring machines (TBM) are favored for large-scale projects in urban areas. Even if TBM can minimize surface settlements (Kolymbas 2005), several factors such as over-excavation, TBM design, void formation behind the tail, mortar behavior, guidance, ground loss, and maintenance breaks may still result in substantial ground movements (Lambrughi et al. 2012).

Currently, the control of TBM excavation is based on theoretical models, numerical simulation outcomes, and the expertise of engineers. To conduct precise and comprehensive studies that would improve decision-making for controlling TBM, it would be possible to rely on 3D finite element models (FEM) taking into account the different sources of uncertainty. However, such numerical models typically require many hours of computation. As a result, it is essential to identify faster and hopefully accurate methods that can assist with decision-making and knowledge development throughout a project.

To reduce computational time for complex and reliable FEM incorporating TBM parameters, machine

learning-based metamodels can be used (see, e.g, Liu et al. 2017, Ninic et al. 2018). In this article, we focus on kriging, aka Gaussian process (GP) modelling, for constructing metamodels from a FEM of TBM excavation. GP modelling is probably the most ubiquitous class of metamodels in the domain of computer experiments (see e.g. Kitanidis 1983, Currin et al. 1988), mainly because it yields a flexible class of models (Williams & Rasmussen 2006) and its theoretical properties are well understood (Stein 1999). GP modelling has been used in many applications and many domains such as biology (Yasrebi et al. 2009), civil engineering (Laurenceau & Sagaut 2008), aerospace engineering (Martin & Simpson 2005), etc.

Our main contribution is to assess the performance of GP modelling for tunneling simulation. To this end, we consider a 2D FE parametric model with plane strain assumption and linear elastic soil mechanics (a very simplified representation of reality) that will make it possible to carry out many simulations for validation purposes at a relatively small cost.

In our methodology we seek to evaluate the performance of kriging metamodels when the number of simulations used to build the metamodel varies against several comparison metrics. We also want to compare different open-source implementations for kriging. Finally, we test kriging against several other classical regression methods.

The modelling assumptions will be explained in Section II. In Section III, a sensitivity analysis using Sobol first and total order indices is conducted to identify key input parameters affecting surface settlements. In Section IV, we conduct numerical experiments to assess the performances of GP modelling. In Section V, we provide conclusions about our numerical experiments and discuss future work.

II. 2D FINITE ELEMENT METHOD OF TBM EXCAVATION

A. General assumptions

In this section we present modelling assumptions to build a toy simulator of TBM excavation that will be used for assessing the performances of GP modelling. The toy simulator is based on the study case introduced in Berthoz et al. (2020). The assumptions are as follows.

First, the soil is assumed to be linear elastic. The settlements prediction accuracy depends on the mechanical properties of the soil (Cheng et al. 2007, Jenck & Dias 2004). Complex soil models provide more accurate predictions of surface displacement shape and magnitude but they come at the cost of longer computational time (Migliazza et al. 2009) and expensive laboratory testing (Zhao et al. 2015) due to the numerous parameters required (as for the Hardening Soil Model in Schanz (1999)). Second, the model assumes 2D-plane strain although mechanical phenomena during TBM excavation are 3D in nature (Lambrughi et al. 2012). Third, we assume symmetry and thus neglect the non-symmetrical nature of urban surface as well as soil heterogeneities. Fourth, the model only simulates one TBM phase whereas the final settlement is the result of multiple sequential steps: excavation, support, mortar injection, and lining installation.

The simulations were performed using the ABAQUS 2022 software and a 3-node linear triangular mesh (CPE3) with finer mesh density near the tunnel and coarser mesh further away (Figure 1). The boundary conditions were defined as follows: complete restriction on all directions of displacement at the bottom, restriction on horizontal displacement on the left and right sides, and free field condition on the top.

B. Simulation of TBM excavation

The model uses a force control approach based on the convergence-confinement method. The tunneling process is represented through the following two steps: 1) geo-stress state definition; 2) soil excavation simulation deactivating the excavated soil and applying pressure to support the wall.

The second step simulates the support provided by the TBM or the lining through the application of

TABLE 1. Global model parameters

Parameters	Notation	Unit	Parameter type	Parametric (Y/N)	Value
Excavation Pressure	P_{exc}	kPa	TBM driving	Yes	160
Gradient Pressure	$\Delta_{P_{exc}}$	kPa/m	TBM driving	Yes	15
Tunnel depth	z_{tunnel}	m	Design	Yes	18
Tunnel diameter	D_{tunnel}	m	Design	No	9.17
Surface weight	$q_{surface}$	kPa	Mechanical model	Yes	75
Watertable level	z_{wt}	m	Mechanical model	No	18.5

either a fictive pressure, representing the force of the TBM or the lining on the soil, or a real pressure to represent the mortar injection between the tail and the lining. A gradient is incorporated to account for the self-weight of materials such as the TBM, excavated soil, mortar, lining, and backup train. Parameters values are detailed in Table 1. The reversible nature of the model due to the soil elastic behavior explains the decision to model only two steps rather than all real phenomena.

C. Geological model

Before tunneling the soil stress state is established calculating the vertical and lateral earth pressure. Vertical pressure σ^v is calculated based on the weight of the soil γ_{soil} in either saturated or unsaturated conditions. The lateral pressure σ^h is obtained by multiplying the vertical pressure by the earth pressure coefficient K_0. To simplify analysis, the influence of pore pressure is disregarded, and the soil is assumed to be linear elastic. Accordingly, the stress state of the soil varies as a function of the depth z.

The selection between drained or undrained conditions is determined by considering factors such as soil permeability and TBM velocity. High soil permeability and low TBM velocity results in fully drained conditions Berthoz et al. (2020). When excavating permeable soil situated below the water table, a fully drained condition is maintained and the stress state is determined using the effective stress σ_{eff}.

$$\begin{cases} \sigma^v_{\text{eff}}(z) = \int_0^z \gamma_{\text{soil}}(x)dx - \int_0^z \gamma_{\text{water}}(x)dx\,, \\ \sigma^h_{\text{eff}}(z) = K_0(z).\sigma^v_{\text{eff}}(z)\,. \end{cases} \tag{1}$$

When dealing with soils above the water table or nonpermeable soils below the water table, the stress state is assessed using the total stress σ_t:

$$\begin{cases} \sigma^v_t(z) = \int_0^z \gamma_{\text{soil}}(x)dx \\ \sigma^h_t(z) = K_0(z).\sigma^v_t(z) \end{cases} \tag{2}$$

TABLE 2. Geologic mechanical properties

Geological layers	ID	Ep. (m)	$\gamma(\text{kN/m}^3)$	E (MPa)	ν	K_0	Water conditions	Stress type
Colluvium	COLL (0)	5	18	32	0.3	0.8	Dry	Total
Saint-Ouen Limestone	CSO (1)	2.5	19	120	0.3	0.7	Dry	Total
Beauchamp Sand	SB (2)	2	21	300	0.3	0.6	Dry	Total
Marls and Pebbles	MC (3)	9	20	200	0.3	0.6	Dry	Total
Coarse Limestone	CG (4)	15	21	600	0.3	0.5	Drained	Effective

γ: soil density (unsaturated when above the water table, or saturated otherwise), E: Young modulus, ν: Poisson ratio, K_0: earth pressure coefficient.

Five geological layers are considered as introduced in Table 2. Additionally, a surface weight is applied to simulate the effects of buildings, backfill, and heterogeneities. As in Berthoz et al. (2020), the mean value of the surface weight is taken as equal to the equivalent of 4 meters of backfill.

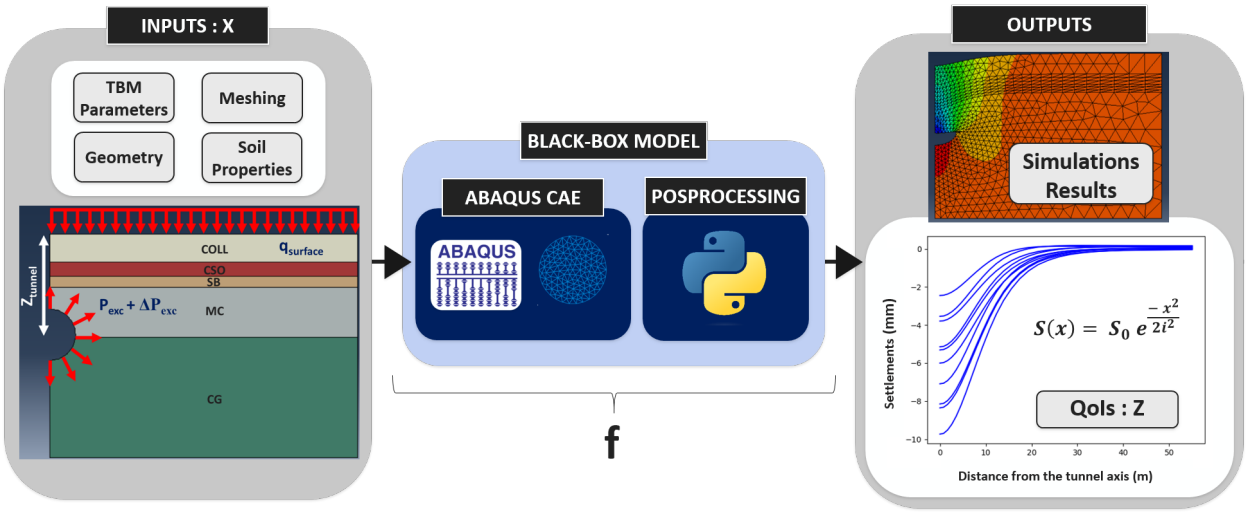

FIGURE 1. Parametric finite element model of the "Paris T6-S6's" tunnel and its black-box representation

TABLE 3. Input random variables of the parametric model

Parameters	Notation	Mean (μ_m)	Coefficient of variation (CV)
Excavation Pressure	P_{exc}	160 kPa	100%
Gradient Pressure	$\Delta_{P_{exc}}$	15 kPa/m	100%
Tunnel depth (surface to tunnel center)	z_{tunnel}	18 m	5 %
Surface weight	$q_{surface}$	75 kPa	30 %
Young Modulus of each geological layer	E	cf Table 2	20 %
Earth pressure coefficient of each geological layer	K0	cf Table 2	20 %

D. Parametric model

A parametric model (Figure 1) has been established to examine the impact of individual parameters on the settlement. Six construction parameters have been selected as inputs. Each parameter is assigned a mean value μ_m and a coefficient of variation (CV) $\delta_m = \frac{\sigma_m}{\mu_m}$ where σ_m is the standard deviation. The values are reported in Table 3.

We also define a domain of variation for each parameter specified as the interval $[\mu_m \cdot (1 - \delta_m), \mu_m \cdot (1 + \delta_m)]$. The mean values and coefficients of variation for pressure and gradient of pressure are based on the findings in Berthoz et al. (2020). For the other parameters, the mean values follow the values used in Berthoz et al. (2020), while the coefficients of variation is set at 20% for soil properties, 30% for surface weight, and 5% for tunnel depth.

A pipeline was established to compute settlements automatically. For a set of input parameters, a simulation is run and the resulting surface settlements (the vertical displacement of nodes at the surface) are recorded as depicted in Figure 1.

To characterize the settlements, two crucial quantities of interest (QoIs) were identified. According to Peck (1969) and other studies, the settlement caused by tunnel excavation follows approximately an exponential curve characterized by two parameters: the inflection point and the maximum settlement. The maximum settlement is estimated by the maximum displacement of surface nodes and the inflection point is determined by fitting a Peck curve to the displacement of surface nodes. Both QoIs are computed and recorded at the end of a simulation.

III. SENSITIVITY ANALYSIS

A. Problem formulation

The finite element model is now viewed as a black box and our objective is to compute Sobol indices (Sobol 1993) to quantify the importance of each input parameter on the variations of quantity of interests (QoIs) that characterize settlements. To this end, we assume that the vector of input parameters is a random vector $X = (X_i)_{i\in[1,d]}$ with uniform distribution $\mathcal{U}(\mathbb{X})$, where $\mathbb{X} \subset \mathbb{R}^d$, $d \geq 1$, is the input domain defined in Section II. D. A given QoI is then a random variable $Z \in \mathbb{R}$ that is computed from the outputs of the FEM presented in Section II. We assume that there is a function $f : \mathbb{X} \to \mathbb{R}$ such that $Z = f(X)$.

B. Sobol indices

Consider the following decomposition of the variance of Z (Efron & Stein 1981, Sobol 1993):

$$V[Z] = \sum_i V[f_i(X_i)] + \sum_i \sum_{k>i} V[f_{i,k}(X_i, X_k)] + ... + V[f_{1,2,...,d}(X_1, X_2, ..., X_d)] \tag{3}$$

with

$$\begin{cases} f_0 = E(Z) \\ f_i(X_i) = E(Z \mid X_i) - f_0 \\ f_{i,k}(X_i, X_k) = E(Z \mid X_i, X_k) - f_i(X_i) - f_k(X_k) - f_0 \\ \dots \end{cases} \tag{4}$$

where $E(\cdot)$ denotes the expectation operator, $E(\cdot \mid \cdot)$ the conditional expectation and $V(\cdot)$ the variance operator. This decomposition exists and is unique under the assumption of independence for the elements of X and other mild conditions established by Sobol (1993). This decomposition leads to the definition of the Sobol indices to analyze the contribution of each input parameter to the variation in the output QoIs Z:

$$S_i = \frac{V[E(Z|X_i)]}{V[Z]}\,, \quad S_{i,k} = \frac{V[E(Z|X_i, X_k)] - V[E(Z|X_i)] - V[E(Z|X_k)]}{V[Z]}\,, \quad \dots \tag{5}$$

The first-order Sobol indices S_i measure the sensitivity of the output random variable Z to a single input random variable X_i. On the other hand, higher-order Sobol indices quantify the variance of the output random variable Z attributed to interactions between multiple input random variables. Additionally, we also introduce the total-order Sobol index:

$$\forall i \in [1, 2, ..., d]\,, \quad S_{T_i} = 1 - \frac{V[E(Z_q|X_{\sim i})]}{V[Z_q]}\,, \tag{6}$$

where $X_{\sim i}$ denotes the random vector in which all components vary except X_i.

The total-order Sobol index S_{T_i} quantifies the combined effect of both the direct influence (first-order index) and the interaction influence (higher-order indices) of input random variable X_i on the output random variable Z.

C. Methodology

A sensitivity analysis using first-order Sobol and total-order Sobol indices is performed on the parametric model described in Section II to assess the impact of each input parameter on the output settlement metrics. The analysis is conducted using the open-source Python framework SALib (Herman & Usher 2017), which employs the Saltelli's sampling approach (Saltelli 2002) to fill the input space $\mathbb{X}$ defined in Section 2.4, using a total of 512 simulation results.

D. Results

Figure 2 displays the first-order and total-order Sobol indices for each input parameter highlighting their effect on the maximum surface settlement and the inflection point of the settlement curve. The analysis

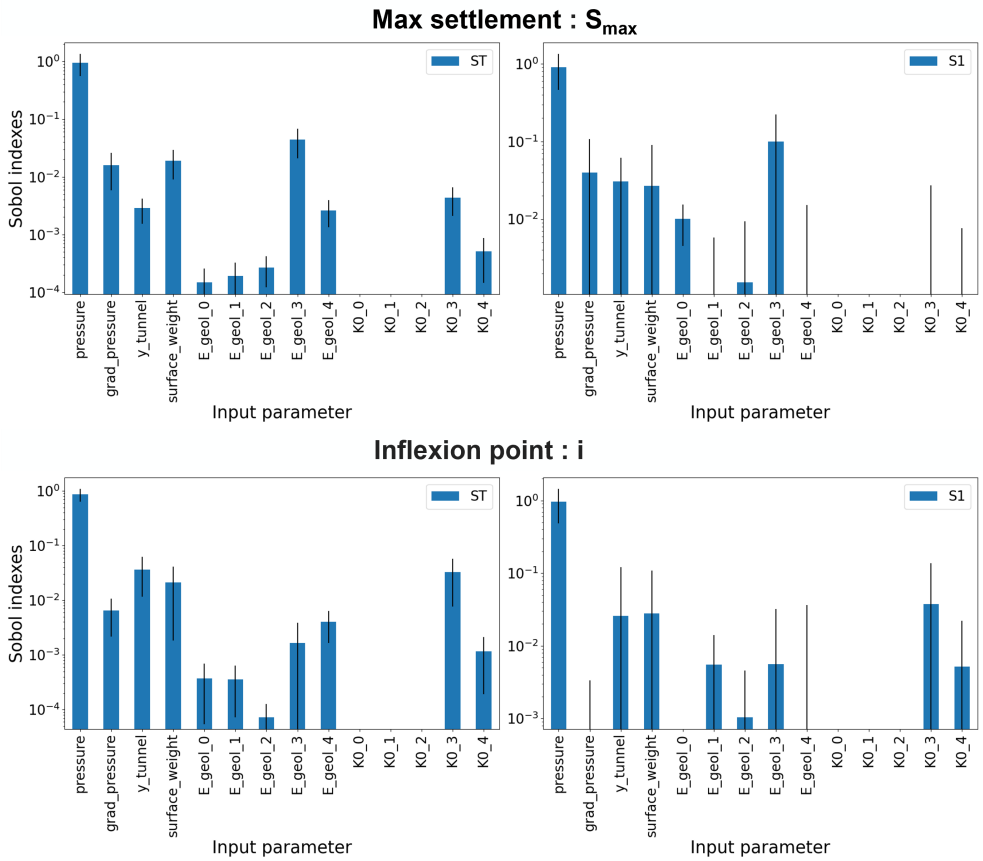

FIGURE 2. Estimating Sobol indices using Monte Carlo simulations
S1: first-order Sobol index, ST: total-order Sobol index. *The blue histogram and black vertical lines correspond to the estimate of the expectation and the 90% confidence interval of the Sobol indices, respectively.*

reveals that excavated pressure has a greater impact on both QoIs than any other input parameter. Moreover, the influence of the geomechanical parameters E and K_0 on the QoIs is significantly greater in the geological layer in which the tunnel is constructed as compared to other geological layers. This finding has practical implications as it suggests the possibility of reducing the number of input parameters and simplifying the problem. In this paper, the input space dimension could be reduced from 14 to 8 by focusing only on the E and K_0 values of the geological layer where the TBM lies.

IV. METAMODEL

A. Kriging

Our objective is to build a cheap approximation of our toy model using kriging, which is more commonly called Gaussian process (GP) modelling in machine learning. Kriging (Matheron 1969) is originally a spatial interpolation technique but it has been applied in the domain of computer experiments for more than thirty years (Sacks et al. 1989). In the following paragraphs we recall the fundamental principles. We encourage the reader to consult reference texts for more details (Chiles & Delfiner 2009, Williams & Rasmussen 2006).

GP modelling is a Bayesian approach where a given QoI depending on the outputs of the black-box simulator is viewed as a GP sample path indexed by input parameters in $\mathbb{X}$. This assumption is denoted by $f \sim \mathrm{GP}(m, k)$, where $m : \mathbb{X} \to \mathbb{R}$ and $k : \mathbb{X} \times \mathbb{X} \to \mathbb{R}$ are the mean and covariance functions of the

GP. The mean function represents the prior expected value (before any simulation) of the unknown QoI as a function of the input parameters $x \in \mathbb{X}$. The covariance function quantifies the prior spatial dependence between the values of the QoIs at different locations in $\mathbb{X}$.

In practice, the user assumes a zero, constant, or linear mean function. The covariance function is usually an anisotropic stationary covariance function written as $k(x, y) = \sigma^2 r(\|x - y\|_\rho)$, $x, y \in \mathbb{R}$, where σ^2 is the GP variance, r is a correlation function, which is often the so-called Matérn kernel in the literature of computer experiments (Petit et al. 2022), and where

$$\|x - y\|_\rho = \Big(\sum_{i=0}^{d} \frac{(x_i - y_i)^2}{\rho_i^2}\Big)^{\frac{1}{2}}$$

is an anisotropic distance depending on a parameters vector $\rho \in \mathbb{R}^d$ called the vector of correlation lengths.

When simulation results $D_n = \{(x_i, f(x_i)), i = 1, \ldots, n\}$ become available, the user uses the GP prior and the data to compute the posterior distributions of $f(x) \mid D_n$ at untried points $x \in \mathbb{X}$.

Under the Gaussian assumption for f, the posterior distribution of $f(x) \mid D_n$ is also Gaussian: $f(x) \mid D_n \sim \mathcal{N}(\hat{f}_n(x), \sigma_n^2(x))$, where $\hat{f}_n(x)$ is the posterior mean, also called the kriging predictor, and $\sigma_n^2(x)$ is the posterior variance, also called kriging variance.

If we assume a zero mean m for f, then $\hat{f}_n$ can be expressed as a linear combination of observed values for the QoIs: for all $x \in \mathbb{X}$, there exists a $\lambda_n(x) \in R^n$ such that $\hat{f}_n(x) = \lambda_n(x)^T \underline{f}_n$, where $\underline{f}_n = (f(x_1), \ldots, f(x_n))^T$. The vector of kriging coefficients $\lambda_n(x)$ corresponding to the posterior distribution minimizes the posterior variance $\sigma_n^2(x)$, which can be written as

$$\sigma_n^2(x) = \mathrm{V}(f(x) - \hat{f}_n(x)) = k(x, x) + \lambda_n(x)^T K_n \lambda_n(x) - 2\lambda_n(x)^T k_n(x), \tag{7}$$

where K_n is the covariance matrix of $\hat{f}_n(x)$ with entries $k(x_i, x_j)$, $i, j = 1, \ldots, n$, and $k_n(x)$ is the covariance vector with elements $k(x, x_i)$, $i = 1, \ldots, n$. Hence, it is straightforward to show that the optimal $\lambda_n(x)$ is the solution of the system of linear equations

$$K_n \lambda_n(x) = k_n(x)\,, \tag{8}$$

which can be computed in $O(n^3)$ operations.

In practice, assuming that the prior mean m is zero is too restrictive. However, kriging can be easily extended to the case where m is written as a linear combination of known functions $\{\phi_l\}_{l \in [0,L]}$.

Finally, it is common to choose the parameters of the covariance function by using a selection criterion. In this work, we use a restricted likelihood criterion, but other criteria are possible Petit et al. (2022).

B. Methodology

A total of $N = 500$ simulations were used to construct random training sets of varying size n. We built a validation set using $M = 100$ simulations. For both sets the space of input parameters, as characterized in Table 3, was filled using Latin Hypercube sampling. Only the input parameters that were found to have an impact on the settlements (see Section III. D.) were selected for this study. Our numerical study aims at:

1. Comparing GP modelling (constant or linear mean, and Matérn covariance) as implemented in `GPmp` (Vazquez 2023) to other regression models implemented in `scikit-learn` (Pedregosa et al. 2011) such as `GaussianProcessRegressor`, `RandomForestRegressor`, `LinearRegressor`, `ExtraTreesRegressor`, and `GradientBoostingRegressor`.

2. Investigating the influence of the size of the train set on the model performance.

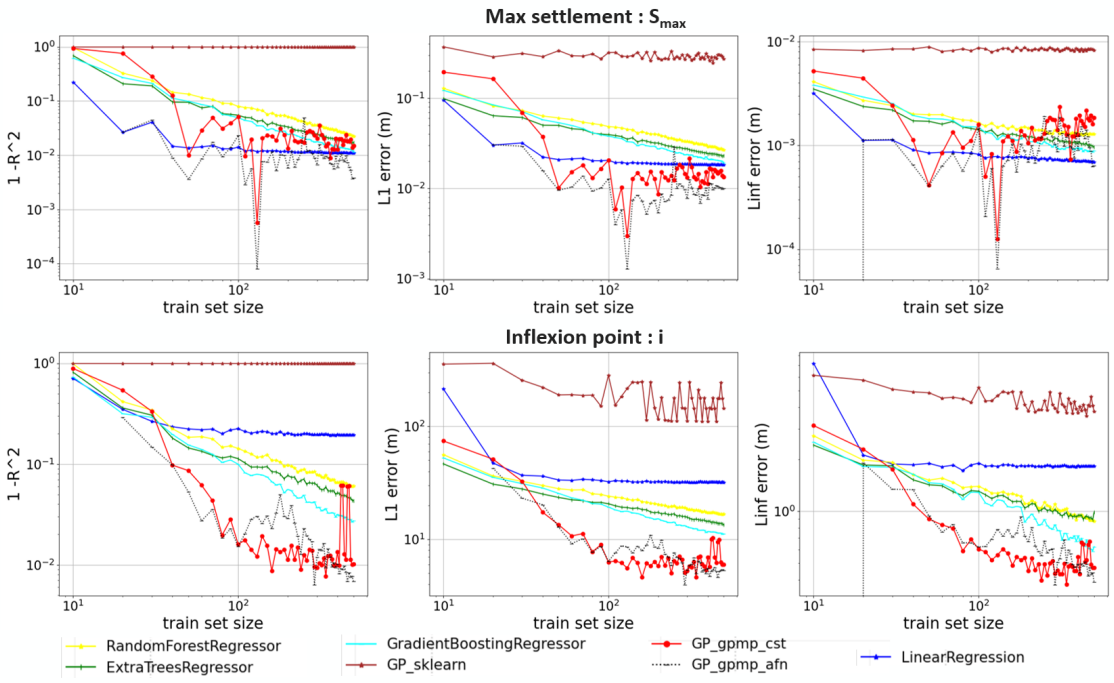

FIGURE 3. Effect of training set size on metamodel performance through $1 - \mathbf{R^2}$, $\mathbf{L_1}$ and $\mathbf{L_\infty}$ error metrics

A total of $K = 20$ models were trained on a randomly selected sample of size n from a training set consisting of 500 data points. Afterwards, each of the K models was tested on an independent test set of 100 data points that were not selected from the 500 data points used for training. The models are compared using three metrics: $1 - R^2$ where R^2 is the coefficient of determination, the L^1 and L^∞ norms of the prediction errors $\varepsilon_{\text{error}} = z_{\text{predicted}} - z_{\text{true}} \in \mathbb{R}^M$. $z_{\text{predicted}}$ and z_{true} stand for the vector of predicted and true values of the QoIs in the validation set.

C. Results

Figure 3 shows that the GP model with constant or linear mean functions implemented using the `GPmp` library outperforms other regression models implemented using the `scikit-learn` framework. The GP regression models exhibit fewer cumulative errors, as indicated by the L^1 metric, and a lower maximum error, as indicated by the L^∞ metric, with an R^2 value that is close to 0.99. In contrast, the GPs regressor implemented using `scikit-learn` has poor performance for the two QoIs.

To summarize, Gaussian Processes (GPs) are highly effective in predicting numerical simulation results making them a suitable approximation method for our TBM problem. While blackbox models in `scikit-learn` can be efficient they may lack transparency, and Gaussian process-based models such as `GaussianProcessRegressor` can be challenging to calibrate. However, GP-based models inherently return a set of solutions with the one chosen being the one that maximizes the restricted log-likelihood. This choice may vary significantly depending on the training space used, leading to high variability in observed performance compared to other approaches. It is worth noting that the scale used to measure this variability is logarithmic, meaning that the actual variation is relatively low.

Nevertheless, it is crucial to keep in mind that achieving good performance with a kriging or other regressor model may require a larger number of simulation points especially when dealing with more com-

plex finite element models. As such, it is essential to carefully evaluate the number and quality of data points used to train the model, particularly if the model is used to make critical predictions or decisions.

V. CONCLUSION

This study shows that metamodels, either using Bayesian or non-Bayesian regressor models, can effectively substitute the 2D finite element model of a tunnel boring machine excavation. Results indicate that a training set of 100 simulation points is sufficient to produce a well-performing predictive model. Furthermore, the Gaussian process regressor using the `GPmp` framework yielded superior results compared to other regression models from the `scikit-learn` package. Using a metamodelling approach may not be necessary for the particular case considered in this article because the simulation time is only about one minute. It would however be highly beneficial for more complex finite element models with multiple input parameters where completing one simulation would take days along with much larger computation resources. Additionally, the sensitivity analysis performed in this study highlights the potential for reducing the number of input parameters to minimize the number of simulation points required to train the predictive model. As a next step, future work will involve implementing a 3D finite element model with a nonlinear soil behavior and generating simulation points to attempt to substitute this model for Gaussian process regressor.

References

Berthoz, N., Branque, D. & Subrin, D. (2020), 'Déplacements induits par les tunneliers : rétro-analyse de chantiers en milieu urbain sur la base de calculs éléments finis en section courante', *Revue Française de Géotechnique* p. 1.

Cheng, C., Dasari, G., Chow, Y. & Leung, C. (2007), 'Finite element analysis of tunnel–soil–pile interaction using displacement controlled model', *Tunnelling and Underground Space Technology* **22**, 450–466.

Chiles, J.-P. & Delfiner, P. (2009), *Geostatistics: modeling spatial uncertainty*, Vol. 497, John Wiley & Sons.

Currin, C., Mitchell, T., Morris, M. & Ylvisaker, D. (1988), A Bayesian approach to the design and analysis of computer experiments, Technical report, Oak Ridge National Lab., TN (USA).

Efron, B. & Stein, C. (1981), 'The jackknife estimate of variance', *The Annals of Statistics* **9**, 586–596.

Herman, J. & Usher, W. (2017), 'SALib: An open-source python library for sensitivity analysis', *The Journal of Open Source Software* **2**(9).

Jenck, O. & Dias, D. (2004), 'Analyse tridimensionnelle en différences finies de l'interaction entre une structure en béton et le creusement d'un tunnel à faible profondeur: 3d-finite difference analysis of the interaction between concrete building and shallow tunnelling', *Géotechnique* **54**, 519–528.

Kitanidis, P. K. (1983), 'Statistical estimation of polynomial generalized covariance functions and hydrologic applications', *Water Resources Research* **19**(4), 909–921.

Kolymbas, D. (2005), *Tunnelling and Tunnel Mechanics: A Rational Approach to Tunnelling*, Springer Science & Business Media.

Lambrughi, A., Medina Rodríguez, L. & Castellanza, R. (2012), 'Development and validation of a 3d numerical model for tbm–epb mechanised excavations', *Computers and Geotechnics* **40**, 97–113.

Laurenceau, J. & Sagaut, P. (2008), 'Building efficient response surfaces of aerodynamic functions with kriging and cokriging', *AIAA journal* **46**(2), 498–507.

Liu, W., Wu, X., Zhang, L., Zheng, J. & Teng, J. (2017), 'Global sensitivity analysis of tunnel-induced building movements by a precise metamodel', *Journal of Computing in Civil Engineering* **31**.

Martin, J. D. & Simpson, T. W. (2005), 'Use of kriging models to approximate deterministic computer models', *AIAA journal* **43**(4), 853–863.

Matheron, G. (1969), *Le krigeage universel*, Vol. 1, École nationale supérieure des mines de Paris Paris.

Migliazza, M., Chiorboli, M. & Giani, G. (2009), 'Comparison of analytical method, 3d finite element model with experimental subsidence measurements resulting from the extension of the milan underground', *Computers and Geotechnics* **36**(1-2), 113–124.

Ninic, J., Koch, C. & Tizani, W. (2018), Meta models for real-time design assessment within an integrated information and numerical modelling framework, *in* 'Advanced Computing Strategies for Engineering: 25th EG-ICE International Workshop 2018, Lausanne, Switzerland, June 10-13, 2018, Proceedings, Part I 25', Springer, pp. 201–218.

Peck, B. (1969), Deep excavation and tunnelling in soft ground, state of the art volume, *in* '7th ICSMFE', Vol. 4, pp. 225–290.

Pedregosa, F., Varoquaux, G., Gramfort, A., Michel, V., Thirion, B., Grisel, O., Blondel, M., Prettenhofer, P., Weiss, R., Dubourg, V., Vanderplas, J., Passos, A., Cournapeau, D., Brucher, M., Perrot, M. & Duchesnay, E. (2011), 'Scikit-learn: Machine learning in Python', *Journal of Machine Learning Research* **12**, 2825–2830.

Petit, S., Bect, J., Feliot, P. & Vazquez, E. (2022), 'Model parameters in Gaussian process interpolation: an empirical study of selection criteria'.

Sacks, J., Welch, W. J., Mitchell, T. J. & Wynn, H. P. (1989), 'Design and analysis of computer experiments', *Statistical science* **4**(4), 409–423.

Saltelli, A. (2002), 'Sensitivity analysis for importance assessment', *Risk analysis* **22**(3), 579–590.

Schanz, T. (1999), 'Formulation and verification of the hardening-soil model', *RBJ Brinkgreve, Beyond 2000 in Computational Geotechnics* pp. 281–290.

Sobol, I. M. (1993), 'Sensitivity analysis for non-linear mathematical models', *Math. Modeling Comput. Exp.* **1**, 407–414.

Stein, M. L. (1999), *Interpolation of spatial data: some theory for kriging*, Springer Science & Business Media.

Vazquez, E. (2023), 'GPmp: the Gaussian process micro package, v0.9.5'. https://github.com/gpmp-dev/gpmp.

Williams, C. K. & Rasmussen, C. E. (2006), *Gaussian processes for machine learning*, MIT press Cambridge, MA.

Yasrebi, J., Saffari, M., Fathi, H., Karimian, N., Moazallahi, M., Gazni, R. et al. (2009), 'Evaluation and comparison of ordinary kriging and inverse distance weighting methods for prediction of spatial variability of some soil chemical parameters.', *Research Journal of Biological Sciences* **4**(1), 93–102.

Zhao, C., Lavasan, A. A., Barciaga, T., Zarev, V., Datcheva, M. & Schanz, T. (2015), 'Model validation and calibration via back analysis for mechanized tunnel simulations–the western scheldt tunnel case', *Computers and Geotechnics* **69**, 601–614.